Rock bolt condition monitoring using ultrasonic guided waves

by B.J. Buys*, P. S. Heyns* and P.W. Loveday†

Synopsis

Rock bolt integrity is a critical issue for the mining industry because of its influence on the safety of mining operations. Guided ultrasonic wave testing of the defects associated with resin-anchored rock bolts was investigated. Axisymmetrical and three-dimensional finite element models were built, one of a partially encapsulated bolt and the other of a bolt with a simulated local corrosion crack. Experimental bolts were then installed in a testing block and typical responses were compared to finite element models of different defect scenarios.

Encouraging results were obtained for the smaller axisymmetrical and three-dimensional finite element models, as well as during the experimental investigation. It is recommended that software with energy-absorbing elements should be utilized to consider higher frequencies and longer bolts. Once the integrity of models such as these has been established, the models could in principle be used to train neural networks for use in commercial equipment to determine the integrity of the installed bolt.

Introduction

Safety is a critical issue for the mining industry. In South African underground mines 1 087 ground fall accidents were reported in 2006 with 85 people killed in these accidents[1]. Much attention is therefore focused on the integrity of the roofs of mining tunnels. One approach is to stabilize the roof with resin-anchored rock bolts. These bolts are essentially steel rods that are fixed into the roof with resin to prevent the roof from collapsing. Supporting the roof with rock bolts is a costly exercise and the quality and density of the support determines the lifespan and reliability of the tunnels[2]. More than 16 million rock bolts are installed each year in South African mines. Of these, 45 per cent are resin-anchored bolts[3].

There are, however, various conditions associated with these resin-anchored rock bolts that might compromise their safety. Examples include weak rock conditions and corrosion, which may cause unsatisfactory bonding between the rock and the rock bolt. Poor installation procedures such as over-spinning, incomplete mixing and partially encapsulated bolts are also encountered[4]. For instance, from 1996 to 1998 approximately half of the fully grouted bolts were reported to be not as effective as they should have been[5,6]. The quality of installation and grouting of resin-anchored bolts is therefore regarded as a serious problem by the mining industry.

Determining rock bolt integrity has been addressed by various groups around the world. One of the conventional approaches to this issue is the pull-out test. However, this is a time-consuming and destructive process. A need therefore arose to develop a non-destructive test that could be used to determine the condition of the bolt *in situ*.

The GRANIT system developed in Scotland drives a piston, which creates a controlled tensile axial impulse that is transmitted to the bolt. The vibration signals arising from this impulse are measured by an accelerometer positioned on the impact device. The acceleration signals arising from this impulse are interpreted by neural networks to determine the condition of the bolt[7]. The disadvantage of the GRANIT system is that it works only on the rock bolts that have been characterized at installation.

Research studies suggest that ultrasonic testing holds the most promise as a non-destructive technique[5]. The Boltometer, which was developed in Sweden, is based on this principle and can be used on grouted bolts as well as polyester and some other resin grouts. The Boltometer uses a sensor with piezoelectric crystals and transmits compressional and flexural waves into the bolt. The

* Dynamic Systems Group, Department of Mechanical and Aeronautical Engineering, University of Pretoria.
† Sensor Science and Technology, Material Science and Manufacturing, CSIR.

Rock bolt condition monitoring using ultrasonic guided waves

waves propagate through the bolt, reflect at the bolt end and the echo is received by the sensor. It relies on the principle that good grouting will absorb most or all of the wave energy into the rock, leaving only small echoes to reach the sensor, whereas insufficient grouting will result in a distinct echo. The Boltometer can indicate bad grouting, but if the impedances of the grout and surrounding rock are the same, wave energy might dissipate into the rock before it could reach a major defect, signalling good grouting[8].

More recently the non-destructive testing of rock bolts using guided ultrasonic waves has been proposed as a feasible approach to detecting resin defects[9]. Guided wave propagation refers to the ultrasonic waves that propagate in solid media with boundaries. These ultrasonic waves experience reflection and refraction with the boundary of the solid, which cause mode conversion between compression and shear waves[10]. Therefore, different guided wave modes can occur in a cylindrical solid. Each of these modes has a particular wave structure. The wave structure describes the distribution of particle motion in the cylindrical solid. Some modes have large particle motion amplitudes near the surface, whereas others feature more intense motion near the middle of the cylinder. The wave structure determines the sensitivity of the particular mode to a particular flaw type. Sometimes it may be possible to perform an inspection using only a single mode. One method of generating primarily a single mode is to employ a Gaussian-windowed, sine burst excitation. The bandwidth of the signal is thus reduced and will suppress modes on either side of the dominant frequency in the frequency spectrum[11].

This approach proposed by Beard and Lowe[9] entails the following: a short duration Gaussian windowed sine burst is used to excite a guided wave in the bolt from the free end. The wave is then reflected from the other end and from any major defects. From the reflection arrival time and knowledge of the wave velocity dispersion curves, the positions of the defects or the bolt length can be calculated. The maximum test range is limited by the extent of the attenuation that the wave experiences as it propagates. The major cause of attenuation for the embedded rock bolt is that ultrasonic energy tends to leak from the bolt into the surrounding rock. With guided waves, the quality of the grouting and the location of the defect can be determined. Specific modes can be selected, which are less sensitive to differences in impedance than the Boltometer.

Beard and Lowe[9] investigated the effect of specific guided-wave modes, frequencies and excitation periods to identify the optimal guided wave mode for detecting defects. Suitable modes and frequencies were selected by means of analytically based dispersion curves, calculated for a simple cylinder. These authors established that embedded bolts should be tested by exciting the first axially symmetrical longitudinal mode known as the L(0,1) mode, in its low-frequency range (30–70 kHz), and the first non-axially symmetrical longitudinal mode known as the L(1,1) mode, in its high-frequency range (2–5 MHz). The low-frequency test can be used to identify defects such as partial bolt encapsulation and possibly corrosion patches near the bolt surface. By contrast, the high-frequency test is not sensitive to surface defects, but can give a reliable indication of the bolt length[9].

This study by Beard and Lowe[9] focused primarily on the identification of suitable modes, which are not significantly influenced by the embedding rock modulus, the epoxy thickness and modulus, and the bolt-epoxy bond quality. Owing to the limitations of the analytical model, it was not possible to simulate complex defect scenarios.

To deal with more complicated defects and geometries, the finite element (FE) method is commonly used to model wave propagation. The primary advantage of the FE method is that there are numerous commercial FE codes available, thus eliminating any need to develop specialized code. Furthermore the finite element method has the advantage that the difficulties associated with complex geometries and defects are simpler to handle. Its availability, user-friendliness and the sophisticated pre- and post-processing options, suggest the finite element method as a versatile modelling approach for rock bolt defect simulation. Different defects such as local corrosion cracking and partially encapsulated bolts can be modelled.

The present study extends the work by Beard and Lowe[9] to investigate damage in more realistic embedded bolts, which deviate from pure cylinders, using the guided wave modes and frequencies suggested by Beard and Lowe. This has been done by using the FE models of various defect scenarios, which are simulated and compared to experimental measurements on bolts. Time traces associated with the different FE defect scenarios could be compared to experimental time traces, which also distinguishes this study from the earlier analytical approach. The present study was limited to lower frequencies because of computer resource limitations. Basic principles and modelling issues could, however, be addressed and it may be expected that these principles could in future be extended to higher frequencies by using a new generation of computers. Once the integrity of models such as these have been established, they could in principle be used to train neural networks for use in commercial equipment.

Exploratory experimental investigations

To develop an understanding of the basic theory and the testing methods involved, the propagation of guided waves in bolts was first investigated experimentally on an unbounded bolt and a perfectly embedded bolt.

These tests were performed using an 18-mm diameter piezoelectric ceramic transducer manufactured by Materials Science and Manufacturing, CSIR (South Africa), cemented to the free end of the bolt. The transducer was a 1-3 piezocomposite disc, which consisted of regularly spaced square pillars of piezoelectric ceramic material supported in an epoxy matrix. The flat surfaces of the disc were covered with silver plating and wires were soldered onto each surface.

A National Instruments PCI 6110 data acquisition card was used to control the transducer. The maximum sample rate on the input channels was 5 MHz. Typically at least 20 samples per period are needed if a good representation of the signal amplitude is required. Therefore, the maximum frequency of interest was limited to 250 kHz. The maximum output voltage of the card was limited to ± 10 V, which necessitated an amplifier. The A-303 Piezo Amplifier from AA Lab Systems was used. This amplifier is a high-voltage, high-speed linear piezo driver. The amplifier is capable of

Rock bolt condition monitoring using ultrasonic guided waves

driving up to ± 200 V at 200 mA at frequencies from DC to 450 kHz. The data acquisition card was driven by Matlab's Data Acquisition Toolbox.

Matlab programs were written to generate different output frequency pulses and to measure the time of arrival. The L(0,1) mode in the low frequency range (30–70 kHz) was excited by applying a Gaussian windowed sine burst voltage to the transducer. Utilizing a number of cycles in the sine burst reduces the bandwidth and results in clearer reflections because the different frequency components of the wave travel at different speeds. This is known as dispersion. This effect becomes apparent when examining the dispersion curves (group velocity vs. frequency plots). The group velocity is the speed at which a packet of waves travel through a solid. The group velocity curve is a familiar curve for guided waves in waveguides, and has its origin in the analytical wave propagation equations. A trade-off study was conducted to determine the most appropriate number of cycles. It was found that fewer than six cycles caused the reflecting signal to become too distorted and more than six cycles might conceal early reflections. It was clear that the optimal number of cycles for the 1.5-m bolt with a testing frequency range of 30–70 kHz, would be a 6-cycle pulse. This resulted in a maximum excitation time of approximately 0.2 ms depending on the frequency. Assuming the speed of the wave packets in steel to be of the order of 5 000 m/s, the defect closest to the free end of the embedded bolt that can be detected is at 0.5 m.

The transducer was connected to an electronic circuit designed to utilize the transducer simultaneously as a transmitter and receiver. The output of the data acquisition card was connected to the amplifier, which in turn was connected to the input of the circuit.

The principle of operation is as follows: when the voltage signal is sent by the data acquisition card, it is amplified by the amplifier before exciting the transducer. The output side of the circuit is connected to the input of the data acquisition card. At the same instant when the transducer is excited, the output side of the circuit also sees this high voltage signal but diodes clip the signal to ± 0.2 V to protect the input of the data acquisition card. The reflections from the embedded end return after a few milliseconds and excite the transducer so that it produces a voltage signal. The voltage of the reflections is smaller than 0.2 V and the signal can be seen on the output side of the circuit. The resistors and diodes were optimized to reduce the noise and expedite the recovery time of the circuit after excitation.

When cementing the transducer, it was attempted to align the disc axis with the bolt axis. The glue was evenly distributed over the surface of the transducer. This was necessary to prevent non-homogeneous bonding to the surface of the bolt, and prevent the transducer from bending and flexural modes from being excited. The amount of glue is also important: the more glue on the surface the greater the energy loss. Any energy loss could not be afforded for the embedded bolt.

It is difficult to find the relationship between voltage and displacement because the exact amplitude of the force transmitted on the experimental bolt cannot be correlated to the excitation voltage, as the quality of the glue bond between the transducer and the bolt affects it. Further research on the transducer and its coupling to the bolt could be expected to improve the repeatability of the experimental results.

Unbounded bolt

A 1.5-m long mild steel bolt with a diameter of 20 mm was suspended in the air on strings to represent an unbounded configuration. The measured voltage time trace for a 40-kHz Gaussian windowed excitation is shown in Figure 1. The amplitude of the excitation signal is much higher than the amplitude of the reflecting signals. The amplitude of the excitation signal was deliberately clipped because the receiving side of the circuit also sees the amplified output signal from the amplifier before it is applied to the transducer. The noise caused by the amplified excitation signal within the instrumentation influences the distance of the defect closest to the free end of the bolt, which can be detected using low-frequency guided waves. The reflections from the embedded end of the bolt can be clearly seen. The group velocities of the unbounded rock bolt model can be compared to the familiar Pochammer-Chree frequency equation[12] which was specifically derived for circumferential waveguides in a vacuum. The speed of a group of waves at 40 kHz, determined from the Pochammer-Chree frequency equation, is around 5 033 m/s, hence the first L (0,1) end reflection should return in 0.6 ms. This is the case for the 40 kHz time trace in Figure 1. Another reflection can be seen between the first L(0,1) end reflection and the second L(0,1) reflection. The speed of the first flexural mode (also known as the F(1,1) mode) at a frequency of 40 kHz is 3 092 m/s. The first end reflection of the F(1,1) mode should return at 0.97 ms which matches the reflection seen in Figure 1. Misalignment of the transducer or non-homogenous bonding of the transducer to the bolt may be the reason that the F(1,1) mode is present. The theoretical attenuation of the F(1,1) mode is approximately 50 dB/m more at 40 kHz than for the L(0,1) mode. The second end reflection will therefore not be visible in the time trace after the cut off time of 1.5 ms shown in Figure 1.

It is evident from the Figure 1 that the arrival times measured compare well to the theoretical values of the velocities of the Pochhammer-Chree frequency equation group. This proves that the experimental setup and FE approach utilized in this study should be adequate to explore more complex defect scenarios.

Embedded bolt

Following the example of Beard and Lowe[9] a concrete block was cast to simulate the effect of an infinite rock mass to test the embedded experimental bolts. This is depicted in Figure 2.

The inside part of the block consists of a mortar core to simulate the sandstone present in the coal and platinum mines in South Africa. The outer part consisting of an aggregate concrete mix was intended to scatter the leaking waves to prevent them from interfering with the waves propagating in the bolt. The size of the mortar block was chosen to ensure that no edge reflections of the block would interfere with the end reflections of the bolt.

To control the introduction of artificial bonding defects accurately and to experiment with different defect scenarios, a fluid type of resin was sought, with a slower reaction time than that used in actual mines. Fibreglass resin was

Rock bolt condition monitoring using ultrasonic guided waves
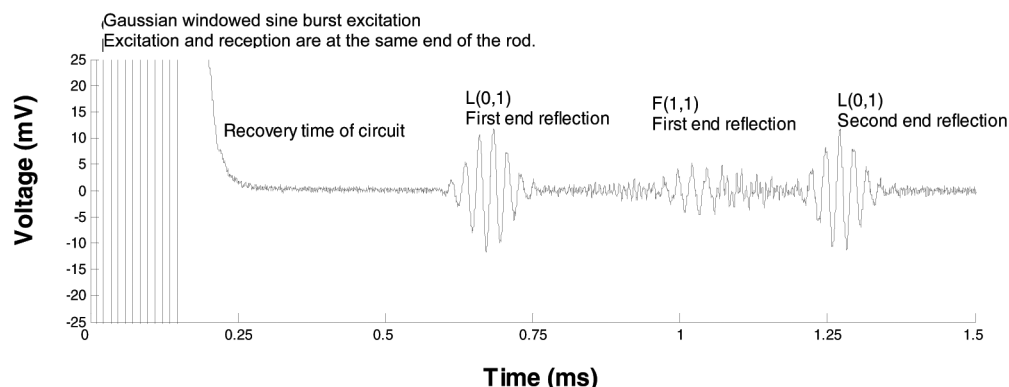

Figure 1—Measured time trace for a 40 kHz Gaussian windowed sine burst excitation of the 1.5-m unbounded bolt
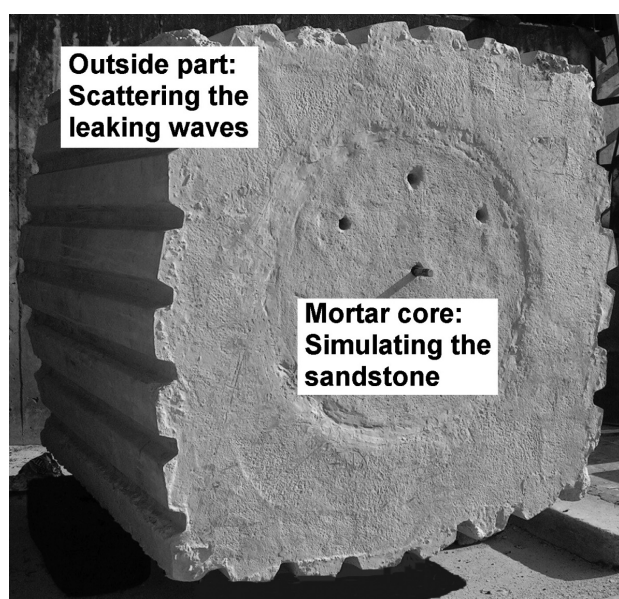

Figure 2—Experimental testing block

eventually selected instead of normal rock bolt resin, because it has basically the same acoustic properties as the rock bolt resin used in the mining industry. This overcame the fast reaction times of normal rock bolt resin and allowed sufficient time for properly controlling the artificially introduced bonding defect scenarios.

Most of the resin-anchored rock bolts installed in the South African coal and platinum mines are between 0.9 and 1.5 m in length[3]. To represent a perfectly embedded bolt, a 0.9 m long mild steel bolt with a diameter of 20 mm was installed in the testing block. The resin gap was between 4 and 5 mm.

The L(0,1) mode was again excited in the bolt using a Gaussian windowed sine burst. The first end's reflection of the L(0,1) mode returned at 0.4 ms as shown in Figure 3. In comparison to the unbounded bolt described in paragraph 2.1, the amplitude of the reflecting signal of the embedded bolt is much smaller than the reflecting signal of the unbounded bolt. This is due to the leakage of the waves into the surrounding rock.

However, the end reflections could be clearly measured for the simple unbounded and embedded bolt configurations considered here. It is evident that the experimental set-up is adequate to explore the effects of more complex defect scenarios.

Finite element modelling of guided waves

Guided wave propagation in rock bolts could be modelled by using full three-dimensional models or axisymmetrical models. Assuming the axial symmetry of the geometry, load, boundary conditions and materials, the axisymmetric model allows one to analyse the three-dimensional bolt and surrounding rock mass with a two-dimensional model.
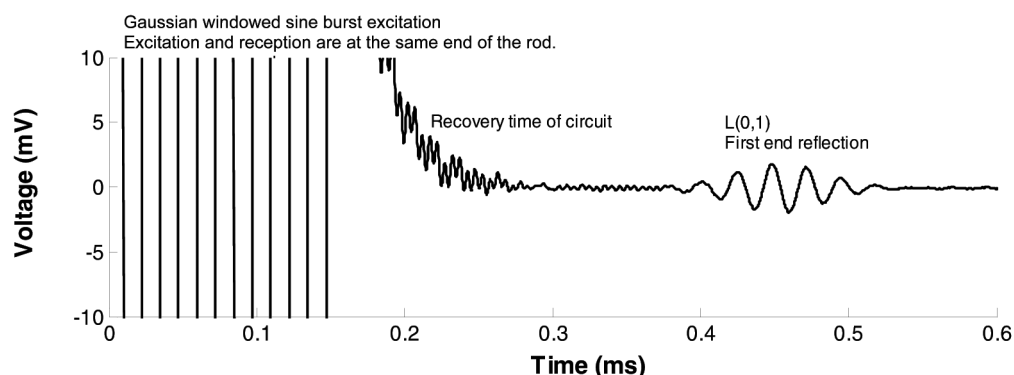

Figure 3—Measured time trace for a 40-kHz Gaussian-windowed sine burst excitation of the 0.9 m embedded bolt

However, defects can occur which are not symmetric around the axis. In such a case a three-dimensional model of the rock bolt will be necessary.

Choosing an appropriate integration time step and element size is critical to the success of the FE solution. In general, the accuracy of the model can be increased by increasingly smaller integration time steps. When the time steps are too long, the high frequency components are not adequately resolved. By contrast, time steps which are too small are a waste of calculation time. The size of the elements is chosen in such a way that the propagating waves are spatially resolved. Suggested time intervals and element sizes for an implicit integration scheme are as follows:[13]

Time step size

$$\Delta t = \frac{1}{20 f_{max}} \qquad [1]$$

Element size

$$L_e = \frac{L_{min}}{20} \qquad [2]$$

where f_{max} is the maximum frequency of interest, and L_{min} is the minimum wavelength involved.

The MSC.Software package, comprising MSC.Patran, MSC.Nastran and MSC.Dytran, was used with a 3.2 GHz Pentium 4 computer and 3 GB of RAM. This allows access to an explicit, as well as an implicit solver.

The effect of mesh density and time step size of the implicit and explicit solvers used were investigated. Different models of the unbounded bolt were built with different mesh densities and time step sizes. The group velocity of each of the models was determined and compared. It could be concluded from the investigation that for the implicit solver, the time step size is more critical than the element size, whereas for the explicit solver, the element size is more critical than the time step size.

Damping is an important factor when doing transient analysis. It does, however, complicate the equation of motion and drastically increases the time required to solve the system of equations. Since Beard and Lowe[9] state that the extent of the amplitude reduction caused by damping is much smaller than the amplitude reduction caused by leakage in the embedded bolt, this study excluded damping to allow for the consideration of larger models. However, excluding damping in the FE model prohibits transients from decaying as time progresses (as will later be seen when comparing FE to the measured results). Investigation of the effects of damping in the finite element models is recommended for future research.

Another modelling issue which had to be addressed was the boundary of the FE model. The finite boundary of the FE model of the rock mass causes the leaking waves to be reflected and superimposed on the progressing waves in the bolt. This problem can be overcome by using energy-absorbing boundaries. This type of element is, however, only available in specialized wave propagation FE packages. The approach used in this study was therefore to move the boundary a large distance away from the bolt so that the boundary would not influence the results[14]. This, however, causes the model to become very large and consequently time consuming to solve, limiting the present study to the low-frequency scenario which resulted in smaller problems than those in the high-frequency scenario. But, as stated before, the basic principles and modelling issues can be studied by considering the low-frequency scenario. It may be expected that a new generation of computers will make it practically feasible to model the high-frequency scenario.

Unbounded bolt

To verify the FE model and to understand the principles of guided wave modelling, the first study undertaken was a model representing an unbounded rock bolt. The rock bolt model was an axisymmetric model with dimensions of 10 mm × 1 500 mm representing the 1.5-m long, 20-mm diameter rock bolt as considered earlier. This model is shown in Figure 4. In its low-frequency band the L(0,1) mode has an axial displacement profile which makes it possible to excite the entire edge of the model at once. A time-varying pressure (Gaussian windowed sine burst) was applied at one end of the model. The element sizes and time step size were calculated according to Equations [1] and [2]. For example, the velocity of a packet of waves at 40 kHz is around 5 000 m/s and the model should have 5 000/(20×40000) = 6.25 mm axisymmetric TRIA 6 elements and the time step size should be 1/(20×40000) = 1.25 µs. The first end's reflection will return at 3/5000=0.6 ms. To see the first and second end reflections clearly, the total time should be set to 1.5 ms. Therefore with a time step size of 1.25 µs a total number of 1 200 time steps should be used. The material properties used for the mild steel throughout the study were: Young's modulus of 206 GPa, a Poisson's ratio of 0.3 and a density of 7 850 kg/m³.

Figure 5 indicates the displacement time trace for the axisymmetric model of the unbounded bolt. It appears that the reflecting signals in the FE model have double the amplitude of the excitation signal, because the edge node sees the ingoing signal as well as the outgoing signal. The F(1,1) mode cannot be modelled with an axisymmetric model. The peaks of the wave packet can be used to calculate the velocity of a packet, which is also known as the group velocity. The next section discusses the way that the group velocity curves for the unbounded rock bolt axisymmetric model were calculated and compared to the results from the experiments on the unbounded bolt.

Comparison of group velocity curves of an unbounded bolt

The velocity of a propagating wave is one of the most important parameters in ultrasonic testing. In bulk waves it is
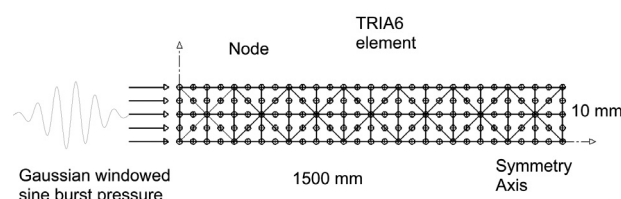

Figure 4—Representation of an axisymmetric model of an unbounded bolt

Rock bolt condition monitoring using ultrasonic guided waves
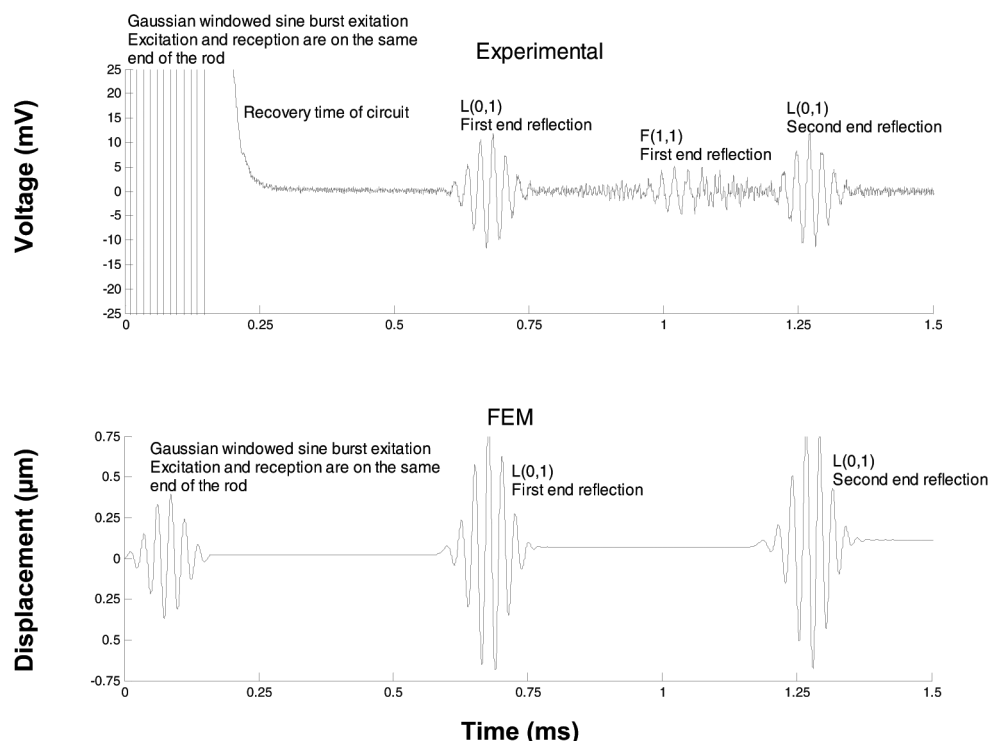

Figure 5—Computed and measured time traces for 40-kHz Gaussian windowed sine burst excitation of a 1.5-m bolt

constant, but in guided waves it changes as the frequency and thickness change and can be represented on a dispersion curve, where the group velocity is plotted against the frequency[15].

To determine the group velocity from a time trace as shown in Figure 5, the time of arrival of a reflection should be measured from the peak of the first wave packet to the peak of the next wave packet. This was done for Gaussian sine bursts over a range of frequencies exciting the unbounded finite element rock bolt model. Different finite element meshes and time step sizes were used as recommended by Equations [1] and [2] for the different frequency bursts.
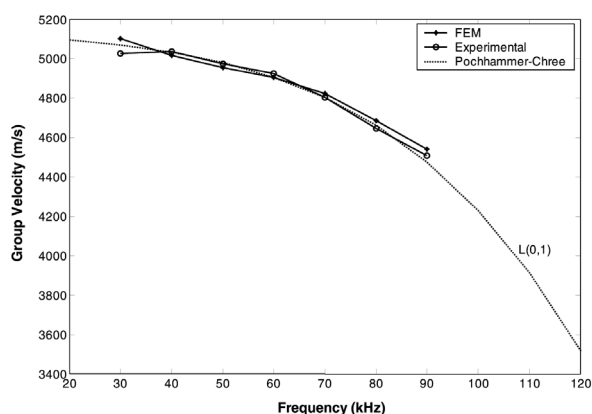
The results obtained from the unbounded experimental

bolt discussed in above were plotted with the results from the FE models and superimposed on the Pochammer-Chree frequency equation. It is clear from Figure 6 that both the experimental and FE results agree well with the Pochammer-Chree frequency equation curve. The maximum difference is 1.2 per cent, demonstrating the potential and accuracy of the finite element method as well as the experimental set-up for simulating more complex defect scenarios.

Defect scenarios

Two main causes of poor anchorage of resin rock bolts are the partial encapsulation caused by poor installation and the cracks formed by local corrosion. These complex scenarios, which deviate from pure cylinders and simple geometries, can be realistically modelled only by finite elements. Axisymmetric models and a three-dimensional model were built and compared to the experimental bolts installed in the testing block. A perfectly installed bolt was also simulated for use as a comparison and reference.

Simulating a fully encapsulated rock bolt

An axisymmetric model was built of a 0.9-m long 20 mm diameter bolt, 5-mm resin bonding and 1-m thick mortar block. The dimensions of the model are shown in Figure 7. The size of the mortar block in the FE model was chosen so as to ensure that no edge reflections of the mortar block would interfere with the end reflections of the bolt. Then 40 to 60 kHz time-varying pressure pulses were applied to the open end of the bolt. Axisymmetric TRIA 6 elements of 5 mm in size were used. It was calculated that reflecting waves would return at 0.343 ms. Using the recommendations

Figure 6—Group velocity curves for the FE model, experimental bolt and the Pochhammer-Chree frequency equation

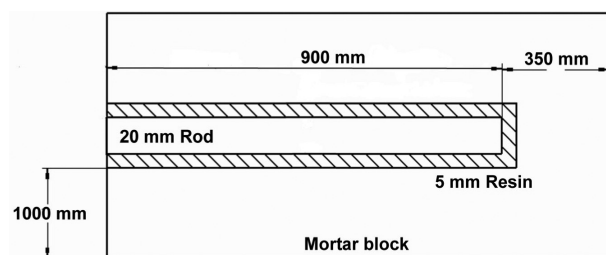# Rock bolt condition monitoring using ultrasonic guided waves

Figure 7—Details of the axisymmetrical model of the fully encapsulated rock bolt

discussed above, the time step was set to 1 μs resulting in 650 time steps. The material properties used for the resin, and mortar throughout the study were: Young's modulus of 10 GPa and 20 GPa, a Poisson's ratio of 0.3 and 0.25 and a density of 1200 and 2500 kg/m³ respectively.

The results obtained for the FE model as well as the experimental bolt for 40-, 50- and 60-kHz pulses are shown in Figures 8 to 10 respectively. For 40-kHz excitation (Figure 8) the first end reflection returned at 0.4 ms. It is notable that the experimental bolt and the FE model show good agreement in terms of identifying the time of the first end's reflection. Furthermore is it noteworthy that the FE response is noisier than the experimental result. This is due to neglected damping, as discussed earlier.

Good agreement was also found for 50 kHz (Figure 9). The attenuation of the signal was lower than in the 40-kHz case. For the 60-kHz pulse (Figure 10) the reflecting amplitudes were even larger than the 40 and 50-kHz pulses. Attenuation due to leakage into the mortar block is therefore lower at the higher frequencies, since at these frequencies the energy travels more in the centre of the bolt.

For a 60-kHz pulse the experimental bolt shows significant reverberation after excitation. This is due to the ringing of the transducer as the transducer is only lightly damped. The ringing was also found by Beard and Lowe in their study[9].

It seems as though a 50-kHz pulse represents an optimal choice between the effects of energy leakage and transducer ringing.

Partially encapsulated rock bolt

Partial encapsulation of bolts anchored in real resin can be caused by improper mixing of the resin and catalyst, where the required spin time is not observed. Underspinning can result in inadequate mixing whereas overspinning can disturb the partially cured resin. Improper mixing can also occur with long bolts where the top of the hole has had less time to mix before the bottom sets. Improper holes that are too deep, too short, too large or too smooth will also result in partially encapsulated bolts. This investigation considered an improper hole scenario where only the end of the bolt was anchored by the resin.

The FE model of the partially encapsulated bolt is shown in Figure 11. An axisymmetric model as well as a three-dimensional model was built. The three-dimensional model was built to investigate the possibility of modelling non-axisymmetric defects.

For the axisymmetric model, the bolt, resin bonding and mortar block were meshed with 5-mm TRIA 6 elements. Then 40-kHz to 60-kHz pressure pulses were applied at the free end of the bolt. The time step size was set to 1 μs and the total number of time steps to 800. It took MSC.Nastran approximately half an hour to solve the problem.

The three-dimensional model of the bolt was built with 5-mm HEX 8 elements. The resin was also modelled with 5-mm HEX 8 elements. The mortar block was modelled with 10-mm HEX 8 elements. With this configuration, the model had approximately 1.2 million elements. The larger elements were necessary to reduce the model to make it solvable. The time step size was set to 0.1 μs and the total analysis time to 0.75 ms. The problem was solved with MSC.Dytran, an explicit solver. It took MSC.Dytran approximately 4 hours to solve this problem.

The results of the experimental bolt, axisymmetric and three-dimensional models are presented in Figures 12 to 14.
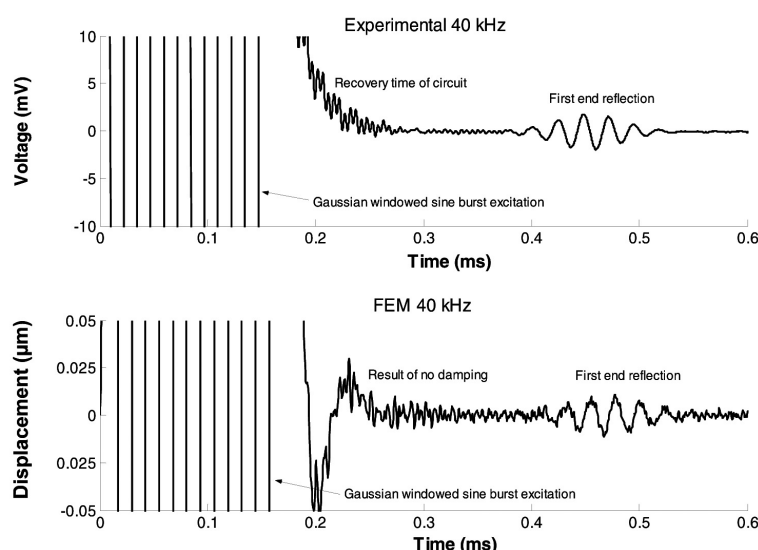

Figure 8—Measured and computed time traces for 40-kHz Gaussian windowed sine burst excitation of the 0.9 m fully encapsulated bolt

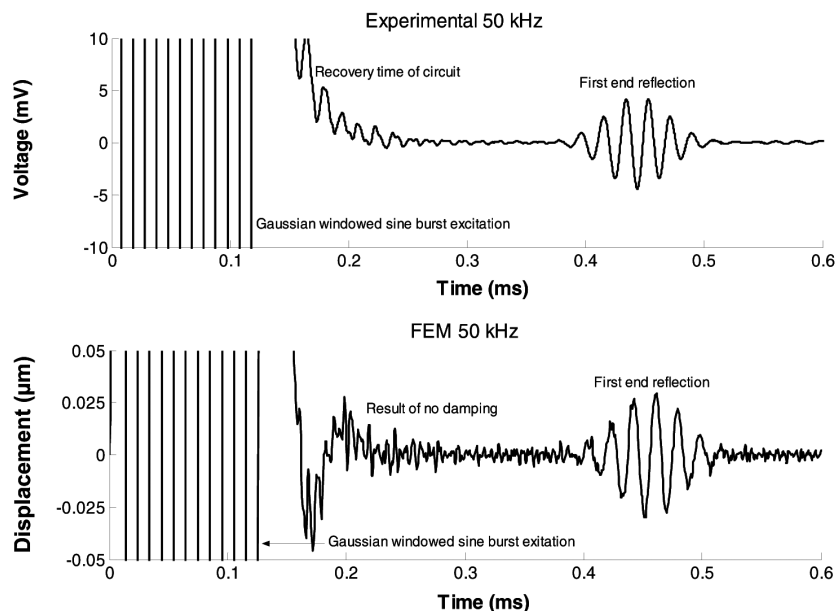# Rock bolt condition monitoring using ultrasonic guided waves

Figure 9—Measured and computed time traces for 50-kHz Gaussian windowed sine burst excitation of the 0.9 m fully encapsulated bolt
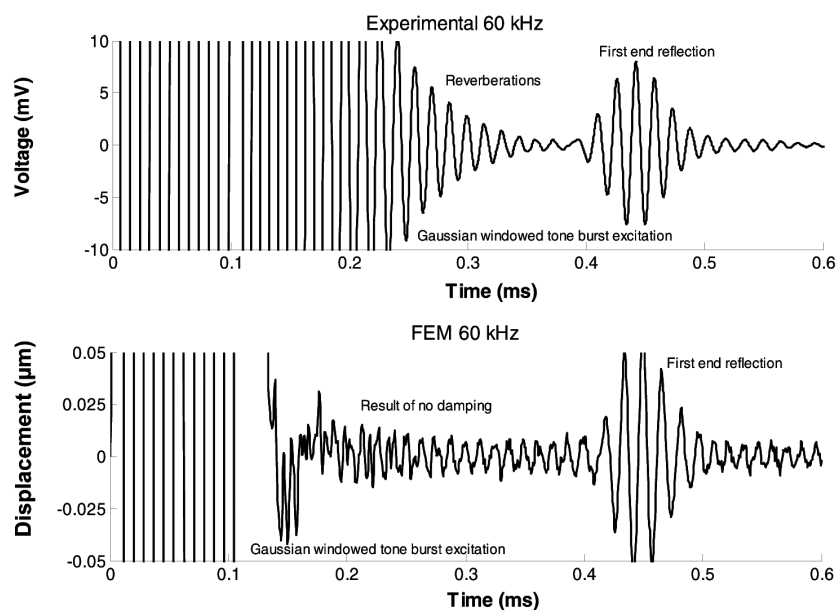

Figure 10—Measured and computed time traces for 60-kHz Gaussian windowed sine burst excitation of the 0.9 m fully encapsulated bolt

The reflection from the start of the resin encapsulation can be clearly seen for the axisymmetric as well as the three-dimensional models for 40-, 50- and 60-kHz excitation pulses. However, on the three-dimensional model the reflected signal becomes stretched out in time for the higher frequencies. At higher frequencies the velocity of the pulse in the concrete causes earlier reflections from the boundary of the mortar block. These reflections interfere with the reflection from the start of the encapsulation, causing the stretched signal. For the higher frequency excitations, the reflections from the start of the encapsulation are smaller than those of the bolt end. This illustrates that more energy propagates in the centre of the bolt at higher frequencies and more energy propagates near the bolt surface at lower
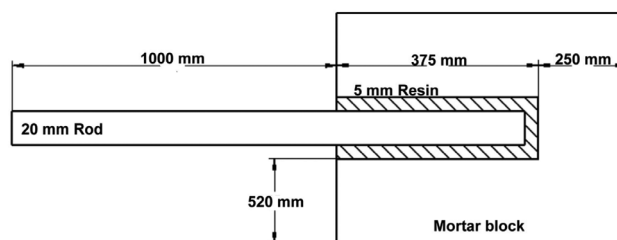

Figure 11—Details of the model of a partially encapsulated rock bolt

Rock bolt condition monitoring using ultrasonic guided waves

frequencies. The reflections from the start of the encapsulation for the experimental bolt also demonstrate that energy travels more in the centre of the bolt at higher frequencies. The difference between the finite element model and the experimental bolt is that the reflections from the start of the encapsulation are much smaller for the experimental bolt. An explanation is that more energy is dissipated in the experimental bolt owing to leakage, which could not be exactly modelled by the FE models because of the uncertainties of the material properties. From the above results, it is concluded that the signal is not significantly influenced by resin defects when the frequency of the signal is high, because the energy propagates more in the centre of the bolt.

Local corrosion cracking

Local corrosion cracking arises from aggressive mineral water seepage through small cracks in the rock and resin, producing metal loss in a confined area of the exposed bolt surface. Ultrasonic guided wave sine bursts were used to investigate different fault scenarios to determine the severity of a corrosion crack. Three crack scenarios were investigated:

- A cracked bolt
- A crack of the resin and rock
- A crack in the bolt, resin and rock.

The dimensions of the model are shown in Figure 15. Only the axisymmetric models were used, as the full three-dimensional model was too large to solve on the computer available. The results of a 50-kHz model are shown in Figure 16.

The reflection from the crack of a cracked bolt can be clearly seen in Figure 16(a). The end-reflection of the bolt is also slightly visible. Most of the energy is reflected back from
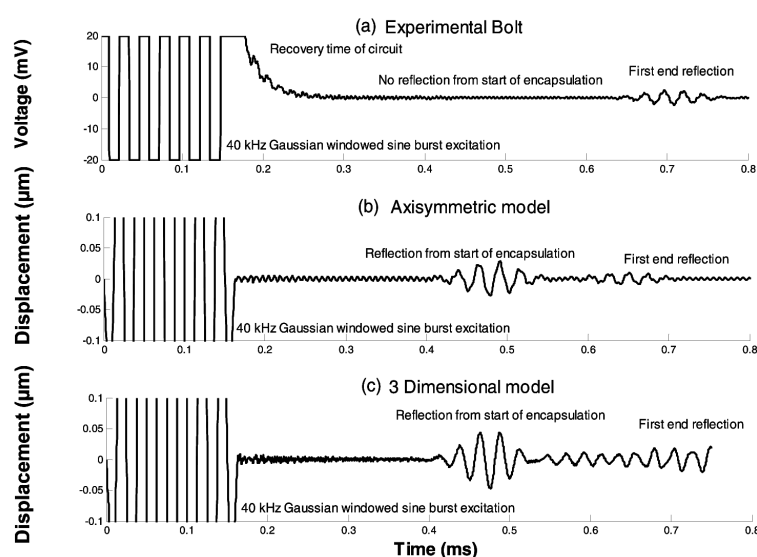

Figure 12—Measured and computed time traces for 40-kHz Gaussian windowed sine burst excitations of the partially encapsulated bolt
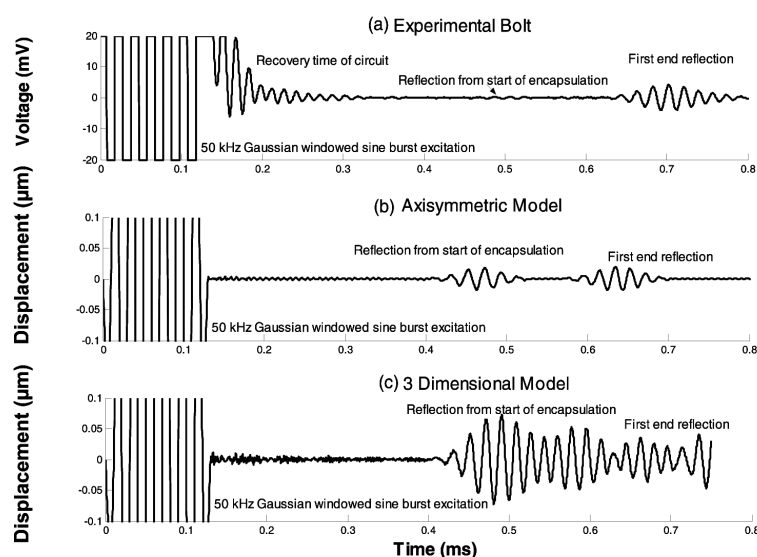

Figure 13—Measured and computed time traces for 50-kHz Gaussian windowed sine burst excitations of the partially encapsulated bolt

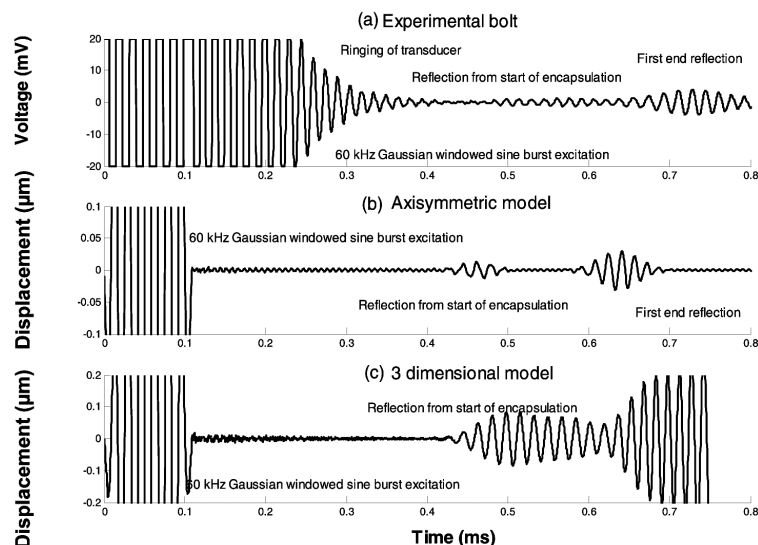# Rock bolt condition monitoring using ultrasonic guided waves

Figure 14—Measured and computed time traces for 60-kHz Gaussian windowed sine burst excitations of the partially encapsulated bolt
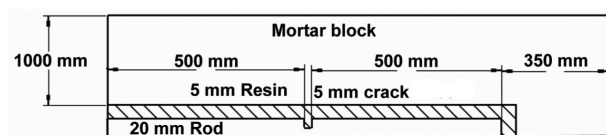

Figure 15—Finite element model: dimensions of the corrosion crack scenarios

the crack, which corroborates the result mentioned above, namely that the energy travels more in the centre of the bolt for the L(0,1) mode.

For the crack in the resin and mortar scenario shown in Figure 16(b), the amplitude of the first reflection is smaller than the reflection of the cracked bolt. This shows that the influence of the resin is not very large for the lower frequency L(0,1) mode.

In the worst case, shown in Figure 16(c) where the bolt, resin and mortar have cracks, the amplitudes of the reflection from the crack in the bolt are larger than those from the crack in the mortar and resin. This again confirms that the energy travels more in the centre of the bolt at these frequencies.

It is clearly possible to detect simulated local corrosion cracks with the finite element models. Clear reflections can be seen from the crack in the bolt. If the bolt, resin and rock are cracked, different reflections are observed. These different reflections complicate the interpretation of the results. Overlapping of returning signals can also further complicate the interpretation of the results. It is therefore recommended that more sophisticated signal processing techniques should be utilized for future studies. For instance, knowing the shape of the exciting signal could help to separate two overlapping reflections.
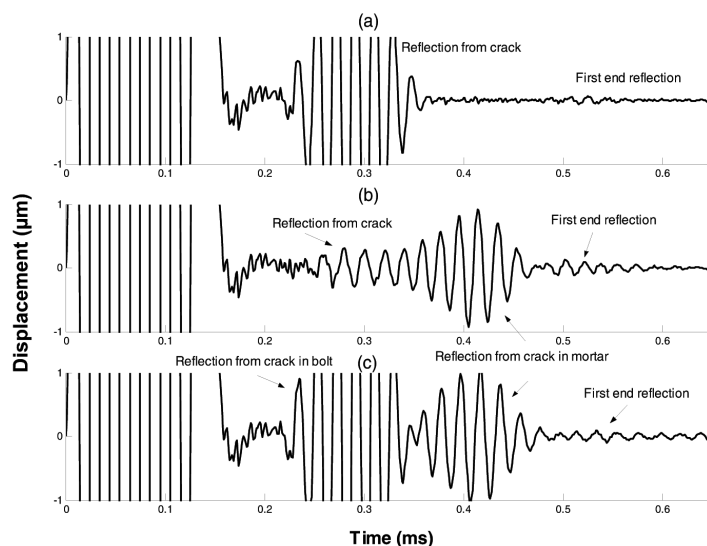

Figure 16—Computed time traces for 50-kHz Gaussian windowed sine burst excitation of corrosion crack scenarios (a), (b) and (c)

Rock bolt condition monitoring using ultrasonic guided waves

Conclusion and recommendations

The use of guided ultrasonic waves for the *in situ* identification of rock bolt condition seems to hold promise as a testing method, as comparable results could be obtained from the experimental and finite element models considered in this study.

The L(0,1) mode in its lower frequency range was utilized and applied, as proposed by Beard and Lowe[9], to investigate the different fault scenarios that can occur in resin-anchored rock bolts.

To gain a fundamental understanding of the above testing method, an unbounded bolt and a perfectly embedded bolt were used as the base reference. The results obtained from an axisymmetrical model of an unbounded bolt compares well with those from the unbounded experimental bolt. The group velocity curves of these models compare well with the group velocity curve of the Pochammer-Chree frequency equation for a rod in air, showing the potential of the method.

Two defect scenarios were then considered. The first was a partially encapsulated bolt. The FE model of this bolt compares well to the experimental results. For the finite element models, the amplitudes of the reflections from the start of the encapsulation are smaller for the higher frequency signals than for the lower frequency signals. It may be concluded that at higher frequencies, the energy propagates more along the centre of the bolt; consequently the higher frequency modes will be less sensitive to partial encapsulation. It is recommended that lower frequencies should be used when defects such as these have to be identified.

It is apparent that it is critical to choose the correct frequency for optimized reflection. When scanning through the frequencies until a reflection from the end of the bolt could be obtained, one could probably select the best frequency for detecting partially encapsulated bolts. However, this should be further investigated.

The second type of defect investigated was simulated local corrosion cracking. It is possible to detect these simulated local corrosion cracks with the finite element models. Clear reflections can be seen from the crack in the bolt. If the bolt, resin and rock are all cracked, different reflections are observed, complicating the interpretation of results. Likewise, an overlapping of returning signals can also contribute to complicating the interpretation of results. It is therefore recommended that due attention be given to signal processing issues in future studies of this nature. For instance, knowing the shape of the excitation signal could help to separate two overlapping reflections. Furthermore, in the case where the local corrosion defects were simulated, only a very simple crack scenario was considered. Further investigations should consider other scenarios, such as inclined and multiple crack scenarios.

This study considered only the time of arrival as a means of locating the simulated defects. However, the amplitude of the reflecting signal may also contain information about the nature and location of a defect. This should be considered in future studies, together with the effect of damping as well as the effect of transducer mounting on the observed responses.

Basic principles and modelling issues were addressed and it can be expected that the basic concepts developed here could soon be extended to higher frequencies with a new generation of computers or by applying energy-absorbing boundaries. The benefit of using higher frequencies is that the higher frequency modes are less sensitive to material properties, epoxy thickness and surface defects. Furthermore the higher frequency modes can be used to obtain a reliable indication of the bolt's length. If the bolt's length is known, the end reflections can be separated from the other reflections, simplifying the interpretation of the complicated reflections of the lower frequency tests. Once the integrity of models such as these has been established, the models could in principle be used to train neural networks for use in commercial equipment.

References

1. SOUTH AFRICAN DEPARTMENT OF MINERALS AND ENERGY—Mine Health and Safety Inspectorate. Annual Report 2006–2007. http://www.dme.gov.za/mhs/documents.stm#3, Accessed 2008-10-12.

2. ROBERTS, D.P. Testing of mining tunnel support elements and systems for hard rock mines. Master's dissertation. Natal: University of Natal. 1995.

3. BORNMAN, H. of Duraset, a South African rock bolt supplier. South African rock bolts consumption. Unpublished e-mail to Buys B.J. (25 April 2005).

4. MARK, C., COMPTON, C.S., OYLER, D.C. and DOLINAR, D.R. Anchorage pull testing for fully grouted roof bolts. *Proceedings, 21st International Ground Control in Mining Conference*, Morgantown, WV, August 6-8, 2002, pp. 105–113.

5. KELLY, A.M. and JAGER, A.J. Critically evaluate techniques for the *in situ* testing of steel tendon grouting effectiveness as a basis for reducing fall of ground injuries and fatalities. Report submitted to SIMRAC, Report No. GAP205, October 1996.

6. HARPER, G.S. and BASSON, E. Develop a new methodology of determining the effectiveness of grouted support. Report submitted to SIMRAC, Report No. GAP412, January 1998.

7. STARKEY, A., IVANOVIC, A., NEILSON, R. and RODGER, A. Using a lumped parameter dynamic model of a rock bolt to produce training data for a neural network for diagnosis of real data. *Meccanica*, vol. 38, 2003, pp. 131–142.

8. THURNER, H.F. Rock bolting—Reference bank, AMFO 84-0847 Final Report. Translated from the Swedish by BC Baur and Associates, Courtesy of CSIR. Johannesburg (Appendix of Kelly A.M., Jager A.J.), Critically evaluate techniques for the *in situ* testing of steel tendon grouting effectiveness as a basis for reducing fall of ground injuries and fatalities, 1996.

9. BEARD, M.D. and LOWE, M.J.S. Non-destructive testing of rock bolts using guided ultrasonic waves. *International Journal of Rock Mechanics & Mining Sciences*, vol. 40, 2003, pp. 527–536.

10. ROSE, J.L. *Ultrasonic waves in solid media*. Cambridge. Cambridge University Press, 1999.

11. CLIFFORD, B. Ultrasonics for integrity testing of rockbolts in mines. Contract Research Report No. 3792/R31.069 prepared by Rock Mechanics Technology Ltd for the Health and Safety Executive, 2000.

12. SECO, F., MARTÍN, J.M., JIMÉNEZ, A., PONS, J.L., CALDERÓN, L. and CERES, R. PCdisp: A tool for the simulation of wave propagation in cylindrical waveguides. *9th International Congress on Sound and Vibration*. Orlando, Florida, 2002.

13. MOSER, F., JACOBS, L.J. and QU, J. Modeling elastic wave propagation in waveguides with the finite element method. *NDT&E International*, 1999, vol. 32, pp. 225-234.

14. ROSS, M. Modeling methods for silent boundaries in infinite media. Fluid-structure interaction aerospace engineering sciences. University of Colorado at Boulder, 2004.

15. STASZEWSKI, W.J., BOLLER, C. and TOMLINSON, G.R. *Health monitoring of aerospace structures*. John Wiley & Sons, Chichester, UK, 2004. ◆

Transaction Paper